On the Link between Mesh Size Adaptation and Irregular Vertices

Daniel Zint[a] and Roberto Grosso[b]

Visual Computing, Friedrich-Alexander Universität Erlangen-Nürnberg, Cauerstr. 11, 91058 Erlangen, Germany

Keywords: Mesh Generation, Block-structured Grids, Irregular Vertices.

Abstract: In numerical simulations and computer graphics meshes are often required to have varying element sizes. High resolution, i.e. small elements, should be only used where necessary. The transition between element sizes requires introducing irregular vertices. In this work, we examine the occurance of irregular vertices in transition regions by setting up an advancing front triangulation that generates optimal transitions. We establish a relation between the appearance of irregular vertices and the properties of the size function and show that a linear transition between different element sizes can be achieved without any singularities on the interior of the transition. Therefore, we can optimize triangulations by setting transition fronts accordingly. These results are used to estimate properties of block-structured grids, e.g. how many blocks are required to represent a given domain correctly.

1 INTRODUCTION

Unstructured and block-structured meshes are widely used in computer graphics and in numerical simulations. They are favored over fully structured meshes due to their adaptiveness to complex geometry. Block-structured grids (BSGs) are on the rise for the last decade. A BSG is a mesh where each element contains a fully structured mesh. In computer graphics BSGs enable tensor product surface representations, grid-based multi-resolution techniques, or discrete pixel-based map representations (Campen, 2017). In numerical simulations, block structure enables optimizations which reduce simulation time drastically. For example, multigrid solvers can be used which converge much faster than solvers that work on unstructured meshes (Armstrong et al., 2015).

Unstructured meshes are irreplaceable in many applications, not just because of their adaptiveness to complex geometry but also for their ability to adapt to a size function. It is well known that there is a link between changes in element size and the appearance of irregular vertices. The more rapid the element size changes the more irregularity is required. Nevertheless, at least as far as we know, this link was never in the focus of research.

In this work, we study the appearance of irregular vertices in transition zones between different element sizes. We describe how irregularities, element quality, and the number of elements are connected. We use this knowledge to achieve optimal transition zones. These are used to remove irregular vertices from meshes that were generated with Delaunay refinement or isotropic remeshing. Furthermore, we gain a deeper understanding about BSG generation. More precisely, we predict the properties of size-adapted BSGs and show constraints that a size function might impose.

1.1 Singularity and Irregularity

The topology of a mesh causes singularities (Beaufort et al., 2017). The Euler characteristic for an orientable surface $\mathcal{S}$ embedded in $\mathbb{R}^3$ is

$$\chi = 2 - 2g - b, \tag{1}$$

where g is the genus of the surface and b the number of boundaries. Thus, for a sphere we have $\chi = 2$, for a disk $\chi = 1$, and for a ring (disk with an interior boundary) or a torus $\chi = 0$. Theoretically, a singularity corresponds to a vertex with no incident edges. In practice a singularity is spread over several vertices. It is more viable to talk about vertex and mesh *irregularity*.

Definition 1. *The* vertex irregularity ι_v *is the vertex valence deducted with its optimal valence. For triangle meshes the optimal valence for interior vertices is* 6 *and for boundary vertices* 4. *For quad meshes*

a https://orcid.org/0000-0003-4491-1685
b https://orcid.org/0000-0001-5965-5325

the optimal valence for interior vertices is 4 *and for boundary vertices* 3.

A vertex in a triangle mesh with valence 5 has an irregularity of $\iota_v = 5 - 6 = -1$ on the interior and $\iota_v = 5 - 4 = 1$ on the boundary. In a quad mesh a valence 5 vertex has an irregularity of $\iota_v = 5 - 4 = 1$ on the interior and $\iota_v = 5 - 3 = 2$ on the boundary.

Definition 2. *The* mesh irregularity ι_m *is the sum of all vertex irregularities,*

$$\iota_m = \sum_{i=1}^{N} \iota_{vi}, \qquad (2)$$

where N is the number of vertices in the mesh and ι_{vi} is the irregularity of the vertex with index i.

Assume the unit square is subdivided in two triangles, Figure 1a. The Euler characteristic is $\chi = 1$. All vertices are on the boundary and thus their optimal valence would be 4. Two vertices have valence 3 giving $\iota_v = -1$ and two have valence 2 which corresponds to $\iota_v = -2$. Therefore, the mesh irregularity is $\iota_m = 2 \cdot (-2) + 2 \cdot (-1) = -6$. This irregularity is purely determined by the topology. We could refine the mesh and flip edges which would create new irregular vertices, but the mesh irregularity will always remain the same as long as the genus or the number of boundaries is not changed, see Figures 1b and 1c.

For investigating transition zones, we need more detailed information about mesh irregularity. We distinguish between positive and negative irregularity.

Definition 3. *The* positive / negative mesh irregularity ι_m^+ / ι_m^- *is the sum of all positive / negative vertex irregularities,*

$$\iota_m^+ = \sum_{i=1}^{N} \begin{cases} \iota_{vi} & if\ \iota_{vi} > 0 \\ 0 & otherwise, \end{cases} \qquad (3)$$

$$\iota_m^- = \sum_{i=1}^{N} \begin{cases} \iota_{vi} & if\ \iota_{vi} < 0 \\ 0 & otherwise. \end{cases} \qquad (4)$$

The unit square has $\iota_m^+ = 0$ and a negative irregularity of $\iota_m^- = -6$. This remains constant if we subdivide the mesh as all new vertices have optimal valence. If edges are flipped, positive and negative irregularity are increased. In Figure 1c we have $\iota_m^+ = 1$ and $\iota_m^- = -7$. Note, that both change equally as they sum up to ι_m,

$$\iota_m = \iota_m^+ + \iota_m^-. \qquad (5)$$

1.2 Irregularity and Quality

Irregular vertices have a negative impact on mesh quality. They impose an upper bound to the minimal

Table 1: Upper bound to minimal quality depending on vertex valence. Quality is measured with mean ratio, minimal angle, and ratio between longest and shortest edge.

valence	q	α_{min}	l_{max}/l_{min}
3	0.60	30	1.73
4	0.87	45	1.41
5	0.97	54	1.18
6	1.00	60	1.00
7	0.98	51	1.15
8	0.94	45	1.31
9	0.90	40	1.46
10	0.85	36	1.62
11	0.81	33	1.77
12	0.76	30	1.93
15	0.65	24	2.40
20	0.51	18	3.20
25	0.42	14	3.99

quality of their incident elements. A common way to measure quality is using the mean ratio metric,

$$q = 4\sqrt{3}\frac{A}{\sum_{i=1}^{3} l_i^2}, \qquad (6)$$

where A is the signed area of the triangle and l_i is the length of its edges (Bank and Smith, 1997; Canann et al., 1998; Amenta et al., 1999). We also consider as quality measures the minimal angle, α_{min}, and the ratio between the longest and shortest edge of a triangle, l_{max}/l_{min}. We only measure minimal quality as for simulations, a badly shaped element might cause numerical instabilities. In contrast, average quality does not contain much information and is therefore neglected.

We compare vertex valence to the optimal minimal quality of its incident triangles, Table 1. This is an upper bound, i.e. a vertex with valence 9 might have a quality of 0.90 but in almost any configuration it will be lower. In the optimal configuration all incident edges have the same length and the same angle between them. Usually, geometric constraints prohibit this setup.

Highly irregular vertices also impose anisotropy. A triangle with a valence four vertex has at best a quotient of longest over shortest edge of 1.41. Depending on the numerical scheme used by a simulation this might not be acceptable.

1.3 Related Work

Adapting to a size function was considered thoroughly in triangle mesh generation methods. The most common procedure is to generate a Delaunay triangulation of a domain and then refine where necessary (Bänsch, 1991; Shewchuk, 1997; Cheng et al.,

(a) Unit Square
$\iota_m = 2 \cdot (-2) + 2 \cdot (-1) = -6$

(b) Refined
$\iota_m = 2 \cdot (-2) + 2 \cdot (-1) + 5 \cdot 0 = -6$

(c) Flipped Edge
$\iota_m = 1 \cdot (-2) + 5 \cdot (-1) + 1 \cdot 1 = -6$
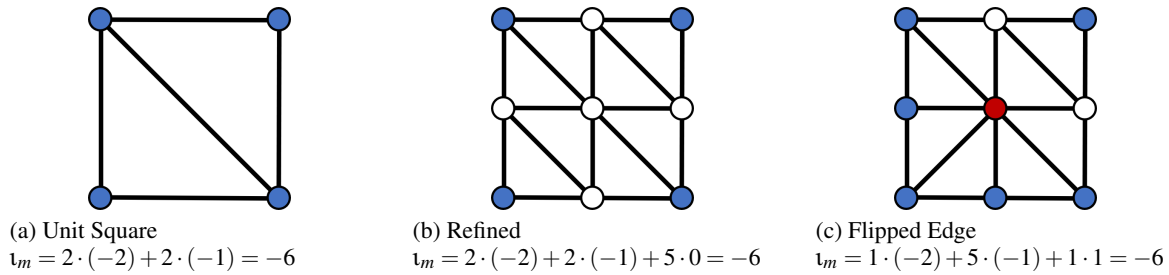
Figure 1: The unit square contains four irregular vertices, two with $\iota_v = -1$ and two with $\iota_v = -2$, summing up to a mesh irregularity of $\iota_m = -6$. Refining the unit square adds five vertices with $\iota_v = 0$. An edge flip affects the vertex irregularity and therefore also the positive and negative mesh irregularity. Vertices with negative or positive irregularity are marked blue or red correspondingly.

2012). Most of this methods add Steiner points to the mesh and flip edges to re-establish the Delaunay triangulation. This iterative approach, called *Delaunay refinement*, is robust and generates unstructured meshes with high quality. *Triangle* is an early software package that used the Delaunay refinement method (Shewchuk, 1996). Subsequent work focused on improving the placement of vertices (Üngör, 2004; Persson, 2005; Erten and Üngör, 2009; Engwirda and Ivers, 2016).

In computer graphics, Delaunay triangulations are generated a bit differently with isotropic remeshing (Botsch and Kobbelt, 2004; Alliez et al., 2008). The steps split, collapse, and smooth are performed subsequently to achieve almost equilateral triangles. Other remeshing methods are based on parametrization (Alliez et al., 2003). Just like Delaunay refinement, remeshing methods can generate meshes with varying element sizes.

Advancing front techniques, sometimes called paving, start at a mesh boundary and add a ring of elements (Peraire et al., 1987; Blacker and Stephenson, 1991; Löhner and Parikh, 1988). This is repeated until the whole domain is filled with elements. Advancing front techniques often deliver good results along boundaries but elements in the interior might have low quality. Advancing front techniques regained interest when they were combined with cross fields and are used especially for quad mesh generation (Remacle et al., 2013; Georgiadis et al., 2017).

None of these methods keeps track of irregular vertices. When the research focus of meshing moved from triangles to quads, irregularities became a topic of bigger concern. Whereas triangles are quite flexible regarding irregular vertices, they are a serious issue in quad meshes due to the lower optimal valence. The introduction of cross fields was an important contribution (Klberer et al., 2007; Ray et al., 2008; Bommes et al., 2009; Bommes et al., 2013; Kowalski et al., 2013; Crane et al., 2010). Cross fields are computed by solving a system of partial differential equations on the domain. Besides giving input for advancing front techniques, cross fields also show positions of singularities and therefore allow directly the generation of block-structured meshes. A downside is that cross fields are not aware of size functions. For mesh adaptation the grid structure needs to be refined by adding further singularities, e.g. Armstrong et al. presents patterns for multiblock mesh refinement (Armstrong et al., 2018). Zint and Grosso try to overcome the issue of cross fields by using a simplification method on an underlying size function to create blocks of the correct size (Zint et al., 2019). Their claim to representing element size correctly leads to a large number of blocks.

2 TRIANGULATING A TRANSITION ZONE

In this section, we study transition zones between areas of different element sizes. First, we will consider a direct transition which does not add any further vertices. Usually, the length of a transition zone is given and the mesh generator has to find the optimal triangulation. First, we go the other way around and examine the behavior of triangulations when we adapt the transition length. In a second step, we will add fronts in the transition zone. Here, we go back to the original problem and find the optimal triangulation for a given transition length.

The examples are generated with an advancing front method. Therefore, we will use the term front for the vertical lines in a mesh. For example, the unit square consists of two fronts, one on the left and one on the right. Furthermore, transitions are described as patterns. The transition pattern 4:1 has 4 elements on the first front and 1 element on the last. If another front with two elements is inserted in between, the pattern is 4:2:1. The number of elements on the front with index k is denoted by f_k. Thus, the pattern with
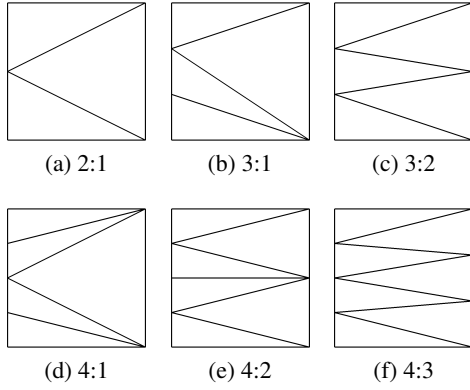
Figure 2: Delaunay triangulation on transition with only two fronts.

four fronts is $f_1 : f_2 : f_3 : f_4$.

2.1 Direct Transition

We use relative irregularity for analyzing transition. This is advantageous as it cancels out the influence of geometry.

Definition 4. *The* relative vertex irregularity $\tilde{\imath}_v$ *is the vertex irregularity in comparison to the unit square as shown in Figure 1a. This only affects the four corner vertices.*

In Figure 2a the top left vertex has $\tilde{\imath}_v = -1$ because in the unit square this vertex has three outgoing edges and here only two. Furthermore, the vertices in the middle and bottom left and the bottom right have $\tilde{\imath}_v = 0$. The vertex in the top right has $\tilde{\imath}_v = +1$. If f_1 is increased, a vertex with $\tilde{\imath}_v = -1$ is added and the irregularity of a vertex on the right side is increased by one, Figure 2b. The opposite happens if f_2 is increased, Figure 2c.

Definition 5. *The* relative mesh irregularity $\tilde{\imath}_m$ *is the sum of the relative irregularity of all vertices,*

$$\tilde{\imath}_m = \sum_{i=1}^{N} \tilde{\imath}_{vi}. \qquad (7)$$

Definition 6. *The* relative positive / negative mesh irregularity $\tilde{\imath}_m^+ / \tilde{\imath}_m^-$ *is the sum of all relative positive / negative vertex irregularities,*

$$\tilde{\imath}_m^+ = \sum_{i=1}^{N} \begin{cases} \tilde{\imath}_{vi} & \text{if } \tilde{\imath}_{vi} > 0 \\ 0 & \text{otherwise,} \end{cases} \qquad (8)$$

$$\tilde{\imath}_m^- = \sum_{i=1}^{N} \begin{cases} \tilde{\imath}_{vi} & \text{if } \tilde{\imath}_{vi} < 0 \\ 0 & \text{otherwise.} \end{cases} \qquad (9)$$

The cases shown in Figure 2 which only consist of two fronts already illustrate some information about transitions:
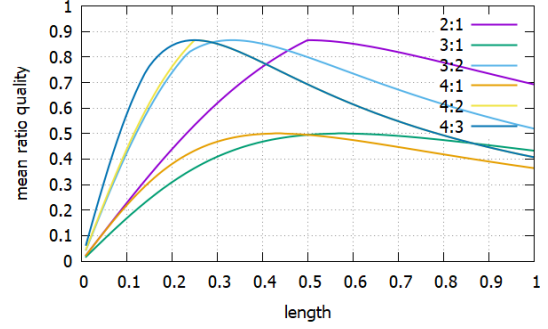
Figure 3: Minimal mean ratio quality of different transitions depending on the transition-length. The domain has a height of 1.

1. The number of elements between two fronts f_k and f_{k+1} is

$$N_E(f_k, f_{k+1}) = f_k + f_{k+1}. \qquad (10)$$

2. The relative positive / negative mesh irregularity is

$$\tilde{\imath}_m^{\pm} = \pm(f_1 - f_2). \qquad (11)$$

3. Negative irregularities are on the first front, positive on the second. Or more general, negative irregularities are on the front with more elements. This is independent of the triangulation, as long as triangles are not degenerated.

Additionally, we study the element quality in transition regions. We observe that triangle quality decreases when f_1 or f_2 increases. Triangles need to be compressed to make room for others. The quality of the pattern 4:3 in Figure 2f would be higher if the transition zone would be shorter. Each transition pattern has its own optimal length. The minimal element quality of the meshes in Figure 2 when stretched in horizontal direction is plotted in Figure 3. Some transitions always have low quality like 3:1 or 4:1. Here arises the question if we can design such transitions with better shaped elements by adding vertices.

2.2 Transition with Multiple Fronts

In the following, we add additional fronts in between the left and right boundary to allow a smoother transition. Therefore, we generalize the domain description. A domain consists of n vertical fronts with $f_1 > f_2 > ... > f_n$. The region between fronts is triangulated according to the Delaunay criterion. Furthermore, we introduce the relative irregularity of fronts.

Definition 7. *The* relative irregularity $\tilde{\imath}_{fk}$ *of a front f_k is the sum of the relative irregularity of all vertices in this front,*

$$\tilde{\imath}_{fk} = \sum_{v \in f_k} \tilde{\imath}_v. \qquad (12)$$

(a) 4:3:2:1   (b) 4:3:1   (c) 4:2:1
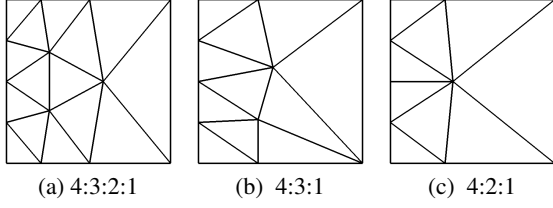
Figure 4: Transition from 4 to 1 element with different patterns.

Definition 8. *The* relative positive / negative irregularity $\tilde{\imath}_{fk}^{+}$ / $\tilde{\imath}_{fk}^{-}$ *of a front f_k is the sum of all relative positive / negative vertex irregularities in this front,*

$$\tilde{\imath}_{fk}^{+} = \sum_{v \in f_k} \begin{cases} \tilde{\imath}_v & \text{if } \tilde{\imath}_v > 0 \\ 0 & \text{otherwise,} \end{cases} \quad (13)$$

$$\tilde{\imath}_{fk}^{-} = \sum_{v \in f_k} \begin{cases} \tilde{\imath}_v & \text{if } \tilde{\imath}_v < 0 \\ 0 & \text{otherwise.} \end{cases} \quad (14)$$

Figure 4 shows different transitions from 4 elements to 1. In Figure 4a two fronts are added. The second front has $f_2 = 3$ elements and the third $f_3 = 2$. Thus, the number of edges is decreased by one between all fronts. The first front (which is the left boundary) has a relative irregularity of $\tilde{\imath}_{f1} = -1$, the second and third front have no irregularity $\tilde{\imath}_{f2} = \tilde{\imath}_{f3} = 0$, and the right boundary has one positive irregularity $\tilde{\imath}_{f4} = 1$. Thus, the additional fronts reduced the relative mesh irregularity from $\tilde{\imath}_m^{\pm} = \pm 3$ to $\tilde{\imath}_m^{\pm} = \pm 1$.

Inserting fronts can be seen as stacking transition zones. In the 4:2:1 example in Figure 4c we have a transition from 4:2 and another from 2:1. The number of elements can be computed as

$$N_E(f_1, f_2, \dots, f_n) = N_E(f_1, f_2) + N_E(f_2, f_3) + \dots$$
$$= (f_1 + f_2) + \dots + (f_{n-1} + f_n)$$
$$= f_1 + f_n + 2 \sum_{i=2}^{n-1} f_i. \quad (15)$$

The first transition generates 2 positive irregularities on the first front and two negative on the second. The second transition generates 1 positive irregularity on the second front and one negative on the third. The positive and one negative irregularity on the second front are canceling each other out giving $\tilde{\imath}_{f2} = 1 - 2 = -1$. This generalizes to the relative irregularity of a front f_k,

$$\tilde{\imath}_{fk} = f_{k-1} - 2f_k + f_{k+1} \quad \text{with } 1 \le k \le n. \quad (16)$$

This holds also for the boundary fronts when we assume that element size is constant outside of the transition zone, i.e. $f_0 = f_1$ and $f_{n+1} = f_n$. From Equation 16 it follows that irregularities only appear when the gradient of the size function is not constant.
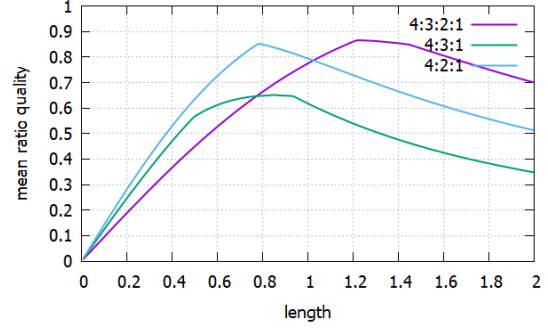
Figure 5: Minimal quality of different transitions between four and one element depending on the transition-length.

With Equation 16 and $f_{k-1} > f_k > f_{k+1}$ for $1 < k < n$ we can compute the relative positive and negative mesh irregularity:

$$\tilde{\imath}_{f1} = f_0 - 2f_1 + f_2 = -f_1 + f_2 < 0 \quad (17)$$
$$\tilde{\imath}_{fn} = f_{n-1} - 2f_n + f_{n+1} = f_{n-1} - f_n > 0 \quad (18)$$
$$\tilde{\imath}_{fk} \ge 0 \quad \text{if } f_{k-1} + f_{k+1} \le 2f_k \quad (19)$$

$$\tilde{\imath}_m^{+} = \sum_{k=1}^{n} \begin{cases} \tilde{\imath}_{fk} & \text{if } \tilde{\imath}_{fk} > 0 \\ 0 & \text{otherwise.} \end{cases} \quad (20)$$

$$\tilde{\imath}_m^{-} = \sum_{k=1}^{n} \begin{cases} \tilde{\imath}_{fk} & \text{if } \tilde{\imath}_{fk} < 0 \\ 0 & \text{otherwise.} \end{cases} \quad (21)$$

$$\tilde{\imath}_m^{+} = \sum_{k=2}^{n} \tilde{\imath}_{fk} \quad \text{if } f_{k-1} + f_{k+1} \le 2f_k \quad (22)$$

$$\tilde{\imath}_m^{-} = f_2 - f_1 \quad \text{if } f_{k-1} + f_{k+1} \le 2f_k \quad (23)$$

Equations 19, 22, and 23 are of special interest as they give hints about optimal transition zones. For the case $f_{k-1} + f_{k+1} = 2f_k$ we can avoid irregularities within the transition zone completely. Thus, the descent in edge size should be equal between all fronts which corresponds to a linear size function. Non-linear size functions will always impose irregularities. Figure 4a shows an optimal transition. Figure 4b and 4c have the same relative mesh irregularity.

In terms of quality, it might not always be the best choice to opt for the lowest possible amount of irregular vertices. Figure 5 shows the minimal quality of the meshes from Figure 4 when stretched along the horizontal axis. The 4:3:2:1 pattern is preferable when the transition is longer. If the transition should be more rapid, the 4:2:1 mesh is the better choice. Thus, depending on the gradient size of a size function one might choose a different pattern. In any case, asymmetric transitions like 3:1 should be avoided as they impose low quality while having the same relative irregularity as symmetric patterns.

(a) remeshing
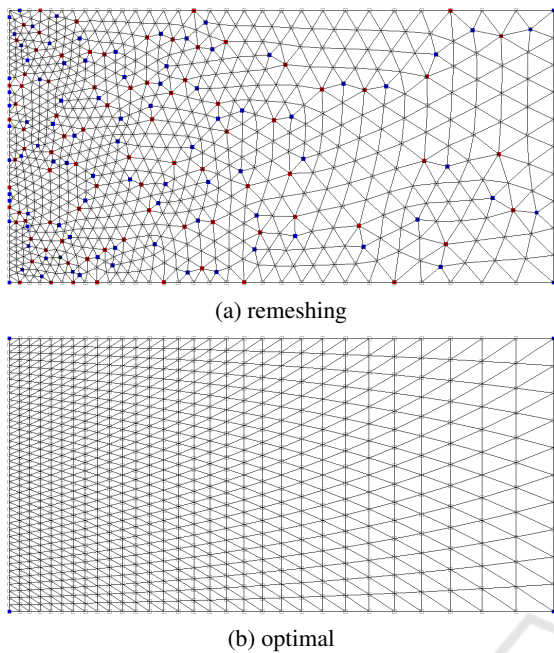
(b) optimal

Figure 6: Transition from 40 to 10 elements once achieved with remeshing, once by computing the optimal transition. Negative irregularities are marked blue, positive irregularities are red.

(a) remeshing   (b) optimal

Figure 7: Transition from 128 to 1 element with an exponential size function once achieved with remeshing, once by computing the optimal transition. Negative irregularities are marked blue, positive irregularities are red.

(a) Delaunay triangulation   (b) optimal
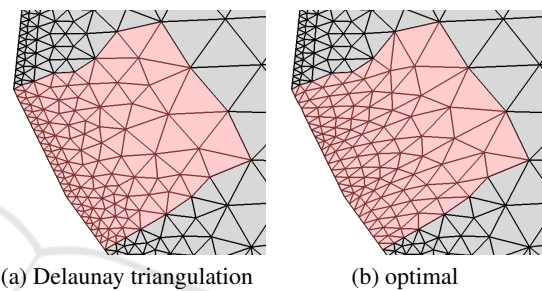
Figure 8: Remeshing a rectangular region in a mesh generated with Delaunay refinement reduces the irregularity significantly.

3 COMPARISON TO ADAPTIVE REMESHING

A simple way to apply a size function to a mesh is by using adaptive remeshing like the one of Botsch and Kobbelt (Botsch and Kobbelt, 2004). Even though remeshing delivers overall good quality, it also generates many unnecessary irregular vertices. In Figure 6a we apply the remeshing of Botsch and Kobbelt to a transition from 40 to 10 elements, assuming a linear size function. The average triangle quality is 0.98 but the minimal quality only 0.39. By computing the optimal transition we only get irregularities on the left and right boundary and achieve a minimal quality of 0.79. The average quality is 0.86. Both meshes have almost the same number of elements, remeshing produces 1 512 and the optimal contains 1 500 elements. In Figure 7, we applied a size function which decreases exponentially. Similar issues are observed here. Remeshing only achieved a minimal quality of 0.33 and an average quality of 0.75 whereas the optimal transition has a minimal and average quality of 0.87. Remeshing generates 313 triangles, the optimal transition has 381.

Also Delaunay refinement can be improved by identifying transition zones and exchanging them with the optimal transition. In Figure 8 we selected a rectangular region of a mesh designed for fluid simulations. Deploying optimal transition reduces the amount of irregular vertices significantly from 63 down to 8. The minimal quality of this region decreases slightly from 0.76 to 0.75. This value could be further improved by smoothing the boundaries of the rectangular region. The number of elements goes down from 205 to 189.

4 PROPERTY-ESTIMATION OF BLOCK-STRUCTURED GRIDS

Optimal transitions can be used to estimate properties of BSGs. Assume, the marked region in Figure 9 should be subdivided into triangular blocks. The region is a transition from 28 to 4 with 10 or 11 fronts. This can be approximated by a relation of 7:1 and one or two interior fronts. Thus, the optimal pattern would be either 7:5:3:1 or 7:4:1, Figure 10. Refining these patterns two times with uniform subdivision results in BSGs with 16 triangles per block that are comparable to the unstructured mesh, Table 2.

The size function imposes that the region should consist of at least 16 blocks. The minimal number of blocks for a 7:1 transition would be 8, but besides
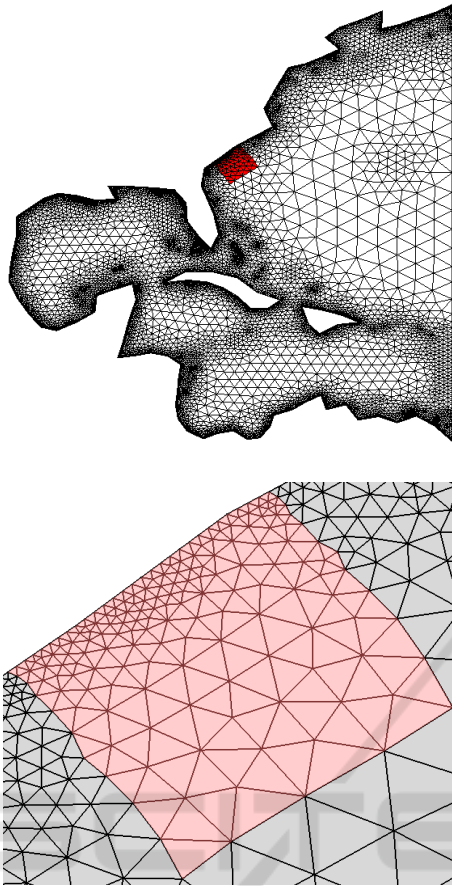
Figure 9: A rectangular transition region within an unstructured triangle mesh. The transition gives information about the number of blocks that is required to represent the domain correctly.

Table 2: BSG property estimation.

	unstructured	7:5:3:1	7:4:1
# blocks		24	16
# triangles	297	384	256
q_{min}	0.75	< 0.98	< 0.90
$\tilde{\iota}_m^+$	40	2	3

generating large irregularities, this would also lead to anisotropy and is therefore not advisable. Also a 7:2:1 pattern would be possible which would then result in 14 blocks but already 16 blocks have less triangles than in the unstructured case. Reducing the number of blocks only makes sense if we can refine the blocks further. This is constrained by the coarsest boundary which only contains four elements. Considering a larger region does not solve this issue as the relation between fine to coarse will remain 7:1.

If 16 triangles build one block, we can compute the number of blocks that is required for representing all 18 578 triangles of the unstructured mesh,

(a) 7:5:3:1   (b) 7:4:1

(c) 7:5:3:1 refined   (d) 7:4:1 refined
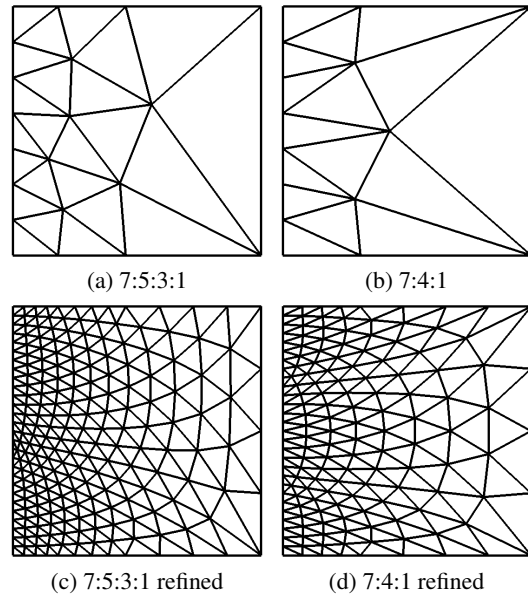
Figure 10: Transition from 7 to 1 element either with one or two additional fronts.

$$n_{block} = \frac{18578}{16} \approx 1161. \qquad (24)$$

This is just a rough estimation but it hints at the minimal amount of blocks. It will not be possible to represent this domain with 10, 100, or even 500 blocks if element size and quality should be preserved.

Depending on the simulation the size function might only be a lower limit, i.e. elements might be smaller but not larger than the value given by the size function. In that case, much less blocks can be generated as the relation between fine and coarse can be set to 4:1 or even 2:1 and blocks may contain more elements than just 16. To enable this transition the number of elements needs to be increased. If one fourth of the triangles would be refined uniformly we would get around 32510 triangles. Assuming that one block would consist of 64 triangles, the mesh could be represented by approximately 510 blocks.

In general, the size function gradient determines the required number of blocks. The larger the gradient the more blocks are required. This issue can not be solved by smoothing as this only adapts the mesh locally.

5 CONCLUSIONS

We studied the transition between different element sizes in triangular meshes. We demonstrated that the minimum number of irregularities in a transition zone can be computed with a simple formula and studied

the influence of irregularities on mesh quality. We also show that a transition requires no interior singularities if the size function gradient is constant. With this knowledge, we can remove irregularities from meshes generated by remeshing or with Delaunay refinement without decreasing quality significantly. Furthermore, we present a technique to estimate the required number of blocks for correctly representing a domain while satisfying the constraints imposed by a size function. In the future, we plan to extend this concepts to more complex problems.

REFERENCES

Alliez, P., De Verdiere, E. C., Devillers, O., and Isenburg, M. (2003). Isotropic surface remeshing. In *2003 Shape Modeling International.*, pages 49–58. IEEE.

Alliez, P., Ucelli, G., Gotsman, C., and Attene, M. (2008). Recent advances in remeshing of surfaces. In *Shape analysis and structuring*, pages 53–82. Springer.

Amenta, N., Bern, M., and Eppstein, D. (1999). Optimal point placement for mesh smoothing. *Journal of Algorithms*, 30(2):302–322.

Armstrong, C. G., Fogg, H. J., Tierney, C. M., and Robinson, T. T. (2015). Common themes in multi-block structured quad/hex mesh generation. *Procedia Engineering*, 124:70 – 82. 24th International Meshing Roundtable.

Armstrong, C. G., Li, T. S., Tierney, C., and Robinson, T. T. (2018). Multiblock mesh refinement by adding mesh singularities. In *International Meshing Roundtable*, pages 189–207. Springer.

Bank, R. E. and Smith, R. K. (1997). Mesh smoothing using a posteriori error estimates. *SIAM Journal on Numerical Analysis*, 34(3):979–997.

Bänsch, E. (1991). Local mesh refinement in 2 and 3 dimensions. *IMPACT of Computing in Science and Engineering*, 3(3):181–191.

Beaufort, P.-A., Lambrechts, J., Henrotte, F., Geuzaine, C., and Remacle, J.-F. (2017). Computing cross fields a pde approach based on the ginzburg-landau theory. *Procedia engineering*, 203:219–231.

Blacker, T. D. and Stephenson, M. B. (1991). Paving: A new approach to automated quadrilateral mesh generation. *International Journal for Numerical Methods in Engineering*, 32(4):811–847.

Bommes, D., Lvy, B., Pietroni, N., Puppo, E., Silva, C., Tarini, M., and Zorin, D. (2013). Quad-mesh generation and processing: A survey. *Computer Graphics Forum*, 32(6):51–76.

Bommes, D., Zimmer, H., and Kobbelt, L. (2009). Mixed-integer quadrangulation. *ACM Trans. Graph.*, 28(3).

Botsch, M. and Kobbelt, L. (2004). A remeshing approach to multiresolution modeling. In *Proceedings of the 2004 Eurographics/ACM SIGGRAPH symposium on Geometry processing*, pages 185–192.

Campen, M. (2017). Partitioning surfaces into quadrilateral patches: A survey. *Computer Graphics Forum*, 36(8):567–588.

Canann, S. A., Tristano, J. R., Staten, M. L., et al. (1998). An approach to combined laplacian and optimization-based smoothing for triangular, quadrilateral, and quad-dominant meshes. In *IMR*, pages 479–494. Citeseer.

Cheng, S.-W., Dey, T. K., and Shewchuk, J. (2012). *Delaunay mesh generation*. CRC Press.

Crane, K., Desbrun, M., and Schröder, P. (2010). Trivial connections on discrete surfaces. In *Computer Graphics Forum*, volume 29, pages 1525–1533. Wiley Online Library.

Engwirda, D. and Ivers, D. (2016). Off-centre steiner points for delaunay-refinement on curved surfaces. *Computer-Aided Design*, 72:157–171.

Erten, H. and Üngör, A. (2009). Quality triangulations with locally optimal steiner points. *SIAM Journal on Scientific Computing*, 31(3):2103–2130.

Georgiadis, C., Beaufort, P., Lambrechts, J., and Remacle, J. (2017). High quality mesh generation using cross and asterisk fields: Application on coastal domains. *CoRR*, abs/1706.02236.

Klberer, F., Nieser, M., and Polthier, K. (2007). Quadcover - surface parameterization using branched coverings. *Computer Graphics Forum*, 26(3):375–384.

Kowalski, N., Ledoux, F., and Frey, P. (2013). A pde based approach to multidomain partitioning and quadrilateral meshing. In *Proceedings of the 21st international meshing roundtable*, pages 137–154. Springer.

Löhner, R. and Parikh, P. (1988). Generation of three-dimensional unstructured grids by the advancing-front method. *International Journal for Numerical Methods in Fluids*, 8(10):1135–1149.

Peraire, J., Vahdati, M., Morgan, K., and Zienkiewicz, O. C. (1987). Adaptive remeshing for compressible flow computations. *Journal of computational physics*, 72(2):449–466.

Persson, P.-O. (2005). *Mesh generation for implicit geometries*. PhD thesis, Massachusetts Institute of Technology.

Ray, N., Vallet, B., Li, W. C., and Lévy, B. (2008). N-symmetry direction field design. *ACM Transactions on Graphics (TOG)*, 27(2):1–13.

Remacle, J. F., Henrotte, F., Baudouin, T. C., Geuzaine, C., Béchet, E., Mouton, T., and Marchandise, E. (2013). A frontal delaunay quad mesh generator using the L ∞ norm. *International Journal for Numerical Methods in Engineering*, 94(5):494–512.

Shewchuk, J. R. (1996). Triangle: Engineering a 2d quality mesh generator and delaunay triangulator. In *Workshop on Applied Computational Geometry*, pages 203–222. Springer.

Shewchuk, J. R. (1997). Delaunay refinement mesh generation. Technical report, Carnegie-Mellon Univ Pittsburgh Pa School of Computer Science.

Üngör, A. (2004). Off-centers: A new type of steiner points for computing size-optimal quality-guaranteed delaunay triangulations. In *Latin American Symposium on Theoretical Informatics*, pages 152–161. Springer.

Zint, D., Grosso, R., Aizinger, V., and Köstler, H. (2019). Generation of block structured grids on complex domains for high performance simulation. *Computational Mathematics and Mathematical Physics*, 59(12):2108–2123.